Available online at www.sciencedirect.com
SCIENCE DIRECT
Progress in Particle and Nuclear Physics 57 (2006) 241–250
Progress in Particle and Nuclear Physics
www.elsevier.com/locate/ppnp

Review

Status of the Germanium Detector Array (GERDA) for the search of neutrinoless $\beta\beta$ decays of ^{76}Ge at LNGS

S. Schönert for the GERDA Collaboration

Max-Planck-Institut für Kernphysik, PO 103980, D-69029, Heidelberg, Germany

Abstract

The Germanium Detector Array (GERDA) for the search of neutrinoless $\beta\beta$ decays of ^{76}Ge at LNGS will operate bare germanium diodes enriched in ^{76}Ge in an (optional active) cryogenic fluid shield to investigate neutrinoless $\beta\beta$ decay with a sensitivity of $T_{1/2} > 2 \times 10^{26}$ y after an exposure of 100 kg y. Recent progress includes the installation of the first underground infrastructures at Gran Sasso, the completion of the enrichment of 37.5 kg of germanium material for detector construction, the prototyping of the low-mass detector support and contacts, the front-end and DAQ electronics, as well as the preparation for construction of the cryogenic vessel and water tank.

Keywords: Double beta decay; Neutrino

1. Introduction

The goal of the Germanium Detector Array (GERDA) [1,2] is to search for the neutrinoless double beta decay of ^{76}Ge. Bare germanium detectors, isotopically enriched in germanium ^{76}Ge, will be operated in liquid nitrogen, or alternatively in liquid argon. The cryogenic fluid serves simultaneously as a cooling medium and as a shield against external radiation. In the case of argon, the scintillation light can be used to discriminate backgrounds. The experiment will proceed in several phases. Phase I encompasses the installation of the experimental infrastructures and the operation of almost 20 kg of enriched detectors in liquid nitrogen, used in the past in the Heidelberg–Moscow and IGEX experiments. With a data sample of 15 kg y and a background of 10^{-2} counts/(keV kg y) the 90% CL limit will be $T_{1/2} > 2.2 \times 10^{25}$ y.

E-mail address: stefan.schoenert@mpi-hd.mpg.de.

0146-6410/$ - see front matter © 2006 Elsevier B.V. All rights reserved.
doi:10.1016/j.ppnp.2005.12.006

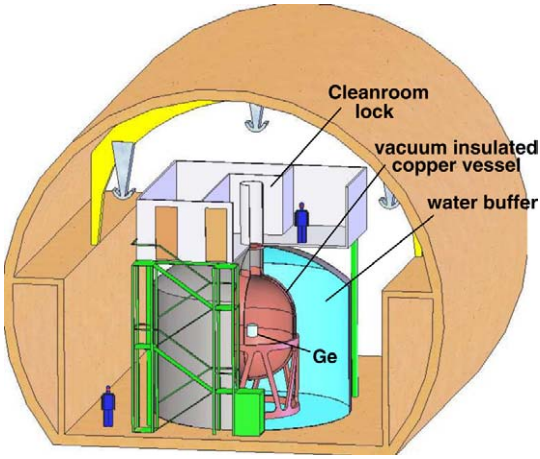

Fig. 1. Schematic view of the GERDA experiment at Gran Sasso.

In Phase II of the experiment new segmented detectors will be added to the setup doubling the target mass. With a background index of 10^{-3} counts/(keV kg y) and an accumulation of statistics of 100 kg y, the 90% CL limit will be $T_{1/2} > 2 \times 10^{26}$ y. This translates to an upper limit of the effective neutrino mass of 0.09–0.29 eV, depending on the nuclear matrix elements used. Depending on the physics results achieved in Phase I and II, a third phase is conceived to reach the 10 meV mass scale. About $\mathcal{O}(1\ t)$ of enriched germanium would be required, which can only be afforded in the context of a world-wide collaboration together with the MAJORANA collaboration [4].

Details of the expected physics performance of GERDA can be found in [1,2]. A schematic overview of the experimental setup in hall A of the LNGS is displayed in Fig. 1.

This paper summarizes the progress of the GERDA project as of September 2005. It is based on the progress report to the scientific committee of the LNGS. A long version of this paper is available [3]. Preparations for the installation have started at the Laboratori Nazionali del Gran Sasso (LNGS). An underground detector laboratory for refurbishing and testing of enriched detectors is now in place. Design and safety reviews for the main infrastructures are currently being carried out. The construction of the main infrastructures underground will commence in 2006.

2. Refurbishment of enriched detectors for Phase I

The refurbishment of the former HDM and IGEX detectors for their use in Phase I of GERDA is under preparation. Characterization and testing of the former HDM detectors with radioactive sources have been completed. The energy resolution of the detectors is the same as, or in some cases even better than, the values published by the HDM experiment. The IGEX detectors are currently stored underground at the Canfranc laboratory. It is planned to move them to Gran Sasso before the end of this year. Test measurements of the detectors in their cryostat using gamma sources will be carried out subsequently at Gran Sasso.

After completion of the testing of the detectors in their cryostats, the germanium diodes will be removed and mounted in new low-mass detector holders. The design of these holders and their contacts has been completed and a first prototype built. Fig. 2 shows some details of the design and a photograph of the prototype detector. The design is optimized to fit the existing HDM and

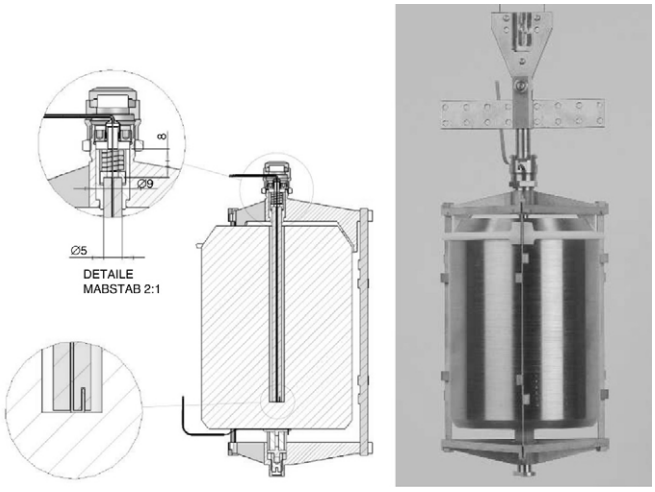

Fig. 2. Left: Drawing of detector support and electrical contacts for Phase I detectors. The signal contact is pressed to the bottom by a pin and a spring, both made out of silicon. Right: Mechanical prototype of a Phase I detector.

IGEX crystals and their particular contact scheme. The inner contact pin and the spring to apply forces onto the pin are made out of single-crystal silicon. Other materials used are NOSV copper from the Nordeutsche Affinerie and PTFE.

The first mechanical and thermal tests with the prototype detector have been completed successfully. The prototype was submerged in liquid nitrogen and all mechanical parts inspected both at liquid nitrogen and room temperature. The next steps include the testing of the electrical contacts using (non-enriched) germanium crystals, as well as a full operational test of a detector assembly. In Monte Carlo studies using the MAGE Geant4 framework, we investigated the background induced by the detector support and contacts. Upper limits obtained from screening measurements with the GEMPI detector were used for copper and PTFE, and those from NAA measurements for silicon. The calculated maximal background due to the holder and electrical contacts is $<1.5 \times 10^{-3}$ counts/(keV kg y)with similar contributions from copper and from PTFE. The design thus meets the specifications of Phase I, i.e. $<1 \times 10^{-2}$ counts/(keV kg y). The materials for the low-background detector support have been procured and are undergoing final screening with the GEMPI detector at Gran Sasso.

3. New detectors for Phase II

The production of new detectors for Phase II is under way. About 20 kg of HP-Ge crystals, enriched in ^{76}Ge, will be fabricated. Germanium enrichment is done by ultracentrifugation of gaseous GeF_4 at the company ECP in Zelenogorsk, Russian Federation. About 37.5 kg of germanium, enriched to a level of 87% in ^{76}Ge, had been produced by September 2005. Enrichment is done in GeF_4, which afterwards is converted to GeO_2. At several steps in the production chain samples for quality control were taken. Various analytical techniques are employed for quality control measurements, among them spark source and glow discharge mass spectrometry (SSMS, GDMS), ICP-MS, and ICP-EAS.

The GERDA collaboration and ECP have co-operated in tuning the employed equipment and re-engineering the handling procedures, in order to maintain the purity of the starting material as much as possible during the entire process. It has been possible to reach a purity of the

enriched material of up to 99.99%, substantially better than the 99.8% which was originally achieved. In addition, by optimizing the batch size the average time where the material remains above ground while enrichment is proceeding could be reduced. The produced batches are stored underground at the ECP site until the entire quantity is enriched. The average time above ground after centrifugation is only 3.1 d, and the storage time underground (ca. 10 mwe) is an average of 120 d.

Preceding crystal growing, chemical purification of the GeO_2 is usually done, before the oxide is reduced to produce 'semiconductor grade' metallic germanium. Tests were performed to see if the higher quality of the enriched material would allow one to skip this step, with negative results. Typically, this purification has a yield of only ≈70%. R&D on chemical purification has led to the development of an improved technique with an expected overall yield of more than 85%.

The enriched material is transported from Siberia to the interim underground storage site by road transport. Transport time from Zelenogorsk to Western Europe is about 3 weeks, depending on road conditions and delay times experienced at border crossings. During transport, the material is stored inside a specially designed protective steel container (PSC). The PSC reduces activation of the germanium by the hadronic component of cosmic rays by about a factor of 10–15. In order to discover possible unforeseen problems and time-delays a 'test transport' with 15 kg of natural (i.e. non-enriched) germanium, was done. Like the 37.5 kg of ^{76}Ge, the 15 kg sample of natural germanium, chemically purified to 99.9999%, was produced in Siberia. It was shipped in exactly the same way as foreseen for the enriched sample. In addition to testing the logistics, the natural germanium sample serves to tune the techniques and instruments employed for material quality checks and as a test batch for crystal production and detector fabrication. Procurement of the natural germanium has been successfully concluded; the natural sample was received at MPI Munich on March 7, 2005 after a 20 day transport time. After unloading of the germanium, the PSC was sent back to ECP in order to be reused for the transport of the enriched material.

For Phase II the germanium crystals will be of "true coaxial" type and have a segmented outer electrode. Detailed Monte Carlo simulations based on Geant 4 have been performed to study the performance of segmented detectors. Segmentation will be 6-fold in ϕ and 3-fold in z, i.e. along the core axis. Segmentation and, in addition, pulse-shape analysis can be used as powerful, complementary tools to reveal the microscopic topology of charge deposition in the crystal, serving to substantially reduce background levels. Background reduction of about one order of magnitude seems feasible by exploiting a combination of both methods.

In the GERDA experiment the detectors are mounted in a modular, scalable arrangement of strings. Each string can hold a maximum of up to 5 detectors. The strings are arranged in a hexagonal structure. The strings are composed of detector units which are individually produced. They are connected to form a string just before loading into the cryostat. A detector unit as depicted in Fig. 3 consists of the following components: germanium crystal, suspension system, HV cable, and segment signal cable.

The suspension system is constructed entirely out of copper and Teflon, similar to that of Phase I. The copper parts provide the main support through a clamp system with two vertical rods, a main holder at the bottom and a stabilizing bar at the top. The detector crystal rests between Teflon pieces. Special Teflon pieces attached to the copper bars allow the fixation of the cables. Samples of all materials are being screened for radioactivity. Limits on the allowable contamination come from Monte Carlo studies. These studies were done using the MaGe framework.

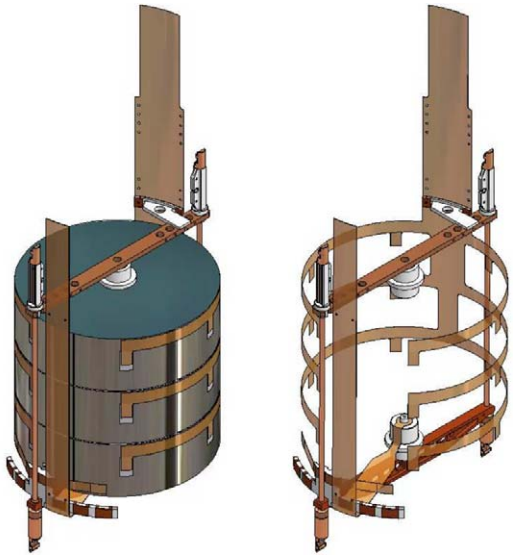

Fig. 3. Left: Detector unit including crystal, suspension and cables. Right: Detector unit without crystal. The segment-signal cable is on the back, the HV-cable is on the front side. Both cables are attached to Teflon pieces which are integrated into the copper suspension.

4. Diode readout and DAQ

Given the limited amount of channels in Phase I of GERDA, it is planned to adopt one of several existing front-end solution. One of the candidate system under test is the hybrid preamplifier [5] +BF862 FET developed in the framework of the AGATA project. It is a hybrid with a BJT devices, and cannot be operated at cryogenic temperatures. The BF862 JFET would be located in a junction box close to the diode at cryogenic temperatures and the preamplifier outside at room temperature. Therefore, for each channel the JFET and its preamp will be connected by two 6 m coaxial cables to close the feedback loop. The performances of the AGATA preamp has been tested with the JFET-preamp distance at 10–20 cm, as well as with a distance of 6 m. The rise times are 6.5 ns and 80 ns respectively. In the latter case, it is necessary either to increase the internal capacitance of the amplifying node of the preamplifier and, consequently, to reduce the bandwidth to eliminate the large ringing of the pulse induced by the propagation delay of the 6 m cable, or to accept the pulse ringing and then to deconvolute the signal using numerical filtering techniques called ‘deoscillation filter’. In both cases, the rise time and equivalent noise charge (ENC) figures are within the GERDA specifications. The deoscillation filter leads to better results for the rise time (33 ns versus 80 ns). For GERDA, it is very significant that the deoscillation method allows one also to reconstruct structures in the rising edge of the input pulse, as shown in Fig. 4. This will allow one to discriminate multi-site events, typical for gamma background, from single-site events characteristically for double beta decay.

In addition the Integrated Pre-Amplifiers IPA4 [6] AMPTEK 250 + SK152 are under study. They can be operated at liquid nitrogen temperatures.

In GERDA Phase II the channel number will increase substantially due to detector segmentation. Therefore, we started to develop ASIC circuits built in CMOS technology, given the improvements in terms of noise obtained with this technique. A circuit having the proper

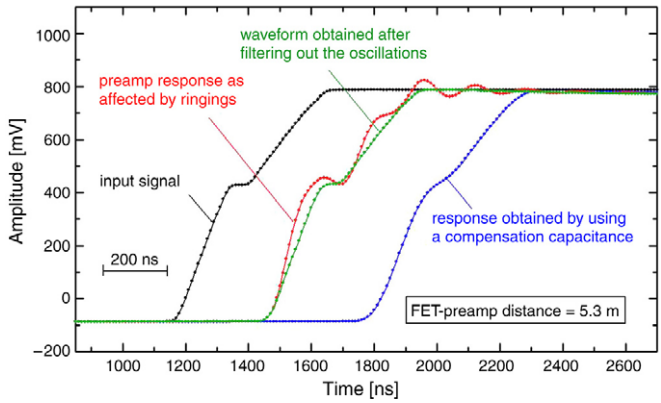

Fig. 4. A pulse with a structure in its rising edge is fed into the uncompensated preamplifier (affected by ringing). The signal shape becomes hardly recognizable. However, it is nicely reconstructed after passing the signal through the deoscillation filter. As a comparison, the signal obtained with a compensation capacitor in the preamplifier is shown.

characteristics to match gamma spectrometry specifications in terms of noise, gain, stability, etc. has been designed at Milano and submitted for production in AMS 0.8 micron technology to EUROPRACTICE. Another CMOS ASIC circuit is currently under development at the ASIC laboratory in Heidelberg.

The analog signals will be fully digitized with FADC system and stored for the off-line analysis. The energy information will be obtained after digital filtering of the signal while the single-site versus multi-site event discrimination will be achieved by analyzing the pulse shape of the recorded charge signal.

Several options for the FADC system have been evaluated. The most promising solutions are the MD^2S system developed by the Padova group of GERDA in the framework of the AGATA project and the commercial VME card SIS3301 of Struck. Even if the performance tests are not fully finalized, both solutions are found to be adequate in terms of analog performance. The SIS3301 is more compact and can also be used for the second phase of the experiment. The MD^2S option is completely developed and offers a cost advantage. The tests also showed that for a long term stability of the system the DAQ has to be housed in a temperature controlled environment.

5. Cryogenic vessel and water tank

The cryostat contains the liquid nitrogen (LN) or argon (LAr) in which the Ge diodes are operated. The cryogenic liquid serves simultaneously as a shield against the remnants of the external γ background penetrating the surrounding water shield and the cryostat's own radioactivity. The baseline is a super-insulated cryostat manufactured predominantly from radiopure ($<19 \times 10^{-6}$ Bq/kg ^{228}Th) copper; the fall-back solution is a super-insulated stainless steel cryostat with an internal lead or copper shield in the cold volume. Basic specifications include an earthquake tolerance of $0.6g$ and a daily evaporation rate of $<0.2\%$.

Fig. 5 shows the almost final layout of the super-insulated copper cryostat. The inner container (KIG) rests on six plastic pads (see detail at lower left); a stainless steel bellow in the neck connects the inner with the outer (KAG) container. Two further sets of radially pointing plastic pads at top and bottom are used to center the inner and outer containers (details in the right part).

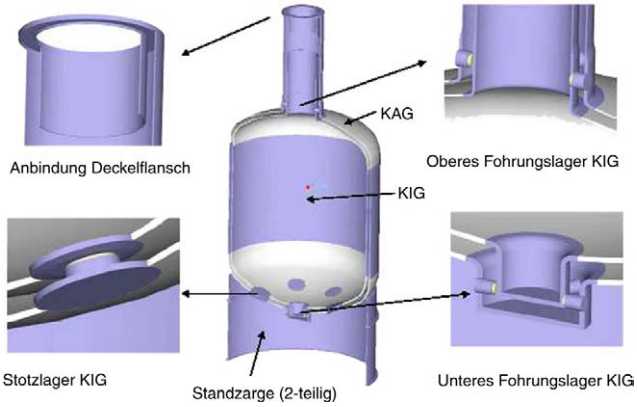

Fig. 5. General layout and some details of the super-insulated copper cryostat.

The alternative design where the inner container is suspended at the neck has been abandoned in order to minimize the stress in the neck. Further improvements as compared to the previous version have been worked out in contacts with the TÜV Nord as well with the manufacturing parties. They include (i) the use of high-purity OFE copper instead of DHP copper as construction material which will yield higher radio purity and better electron beam welding properties, (ii) the exchange of hemispherical heads which would have been welded from eight segments by Korbbogen heads which can be pressed as one piece from a single copper metal sheet, and (iii) the compliance of the design with the framework 'Basissicherheit von druckführenden Komponenten' (BSK — base safety for pressurized components) which is used for the design and construction of German pressurized-water reactors.

The safety review of the cryostat and water vessel system was started in spring 2005 with the preparation of various safety analysis documents. Following several iterations, the GERDA collaboration is currently investigating the insertion of an additional wall between cryostat and water vessel in order to further minimize the risk of mixing cryoliquid and water.

The definitive engineering project of the water tank (WT), together with the construction plan, was completed in July 2005. It will be made in stainless steel (316AL or equivalent). Fig. 6 shows a side view of the water tank, the cryostat, the superstructure, and the lock inside the penthouse as conceived before the third wall recommendation.

In parallel, the design of the laboratory building and of the superstructure was developed. In order to decouple as much as possible the construction of the WT from the completion and insertion of the cryostat, the construction plan foresees initially leaving a part, approximately 4.5 m width $\times$ 6 m height, open for the insertion of the cryostat. After insertion, the construction of the tank will be completed by final welding.

6. MC simulations and background studies

The current MC efforts concerned the evaluation of (i) the cosmic-ray-induced background and optimization of the Cherenkov muon veto, and (ii) the evaluation of the background due to radioactive contaminations in the crystals and in the supporting structures. For space reasons, here we report only results of the first activity. The simulations have been carried out using the Geant4-based MAGE framework, which is developed and updated jointly with the Majorana collaboration.

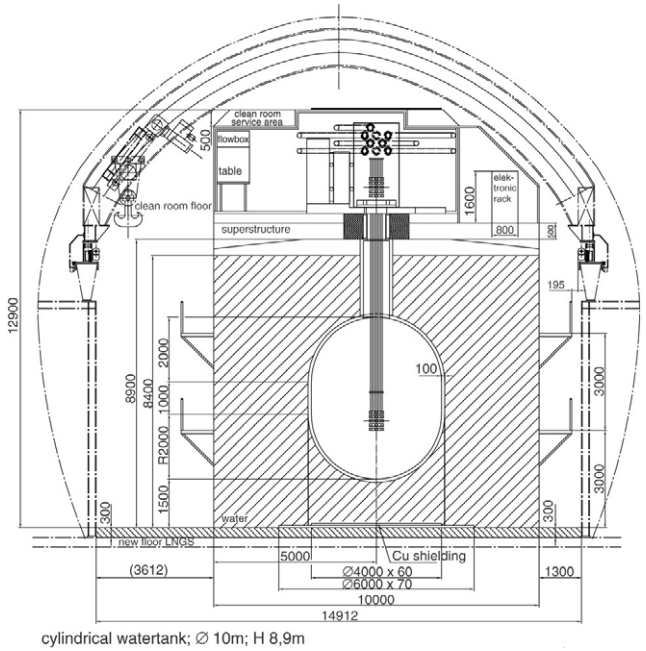

Fig. 6. Vertical cut through the center of the experiment looking from the TIR gallery. The recommended third wall between water and cryostat is not yet shown.

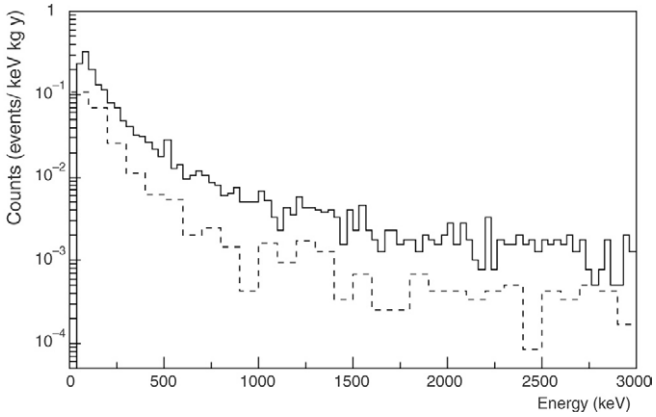

Fig. 7. Muon-induced background for Phase I without (solid) and with (dashed) crystal anti-coincidence.

The contribution of cosmic-ray muons (and of the induced neutrons in the GERDA experimental set-up) to the background index at $Q_{\beta\beta}$ is shown in Fig. 7 and summarized in Table 1 for Phase I. The anti-coincidence cut between the 9 crystals of Phase I can reduce the background of a factor of 4.5, down to 4.1×10^{-4} counts/keV kg y, which meets the goal, 10^{-2} counts/keV kg y. The background index with the Cherenkov muon veto is lower than 3×10^{-5} counts/keV kg y (at 95% CL) for 120 MeV energy threshold, which can be achieved with about 80 PMTs.

Table 1
Background index in the range 1.5 → 2.5 MeV for different veto scenarios

Condition	Background index (counts/keV kg y) Phase I
No cuts	$(1.9 \pm 0.1) \times 10^{-3}$
Crystal anti coincidence	$(4.1 \pm 0.5) \times 10^{-4}$
Anti-coincidence and plastic muon veto	$(3.5 \pm 0.6) \times 10^{-4}$
Anti-coincidence and Cherenkov muon veto	$<3 \times 10^{-5}$ at 95% CL
Anti-coincidence and both muon vetoes	$<3 \times 10^{-5}$ at 95% CL

The threshold for Ge detectors is 50 keV. The quoted errors are the statistical ones.

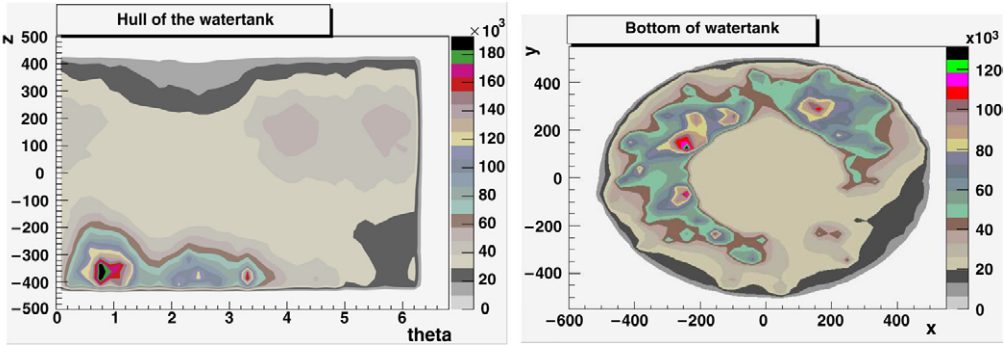

Fig. 8. Cherenkov photon intensity maps for bottom and unfolded hull of the water tank of muon events which have an energy deposition in the germanium crystals in the range 1.5–3.0 MeV. The photons centrally under the cryostat are not shown here.

The optimization of the muon veto system consisting of a plastic scintillator system on top of the water tank and of the water Cherenkov system is ongoing. In the simulations, muons are selected which deposit energy in the germanium detectors. Up to now, about 140 million muons have been simulated, using the Gran Sasso muon distribution. About 20 000 muons of those caused energy deposition in the crystals. Out of those 260 muons were identified as 'dangerous', i.e. the energy deposition in one or more germanium crystals was in the range 1.5–3.0 MeV. For those muons, specific Monte Carlo simulations have been run to reconstruct the photon maps in the water tank and to optimize the placement of the PMTs. For instance, Fig. 8 shows the photon map of the hull and bottom of the water tank. VM2000 is used as a light reflector and wavelength shifter.

Details of the veto trigger have still to be defined, but the results of the MC already show that an efficiency of more than 98% for the dangerous muons can easily be achieved. The plastic scintillator tags with high efficiency muons which enter into the neck and are stopped inside of the cryotank.

7. Material screening

Screening of materials for radioactive impurities is performed by gamma spectrometry, and complementarily with ICP-MS. Another important activity concerns the purity control of argon in terms of ^{222}Rn and the development of purification procedures. Also surface impurity studies are being carried out. Here, we report recent measurements concerning the purity and purification procedures of liquid argon, the alternative for liquid nitrogen in GERDA. We investigated the

initial ^{222}Rn concentration in argon from the German Company Westfalen AG. For argon 5.0 we found a high activity of 8 mBq/m^3 (STP). For the better quality argon 6.0 the initial activity is significantly lower (0.4 mBq/m^3 (STP)). Due to the decay of ^{222}Rn these concentrations decrease with time and are finally given by the ^{222}Rn emanation rate of the specific storage tanks. We have measured the ^{222}Rn saturation activity of two standard cryogenic storage tanks after the cryoliquid had evaporated. The results were 40 mBq and 190 mBq for a 600 liter tank and a 3500 liter tank, respectively. Under the assumption of equally distributed radon in the argon the final ^{222}Rn concentration in the completely filled 3500 liter tank is 0.07 mBq/m^3 (STP). However, we have observed that radon predominantly sticks to cold walls, hence the ^{222}Rn concentration in the argon will even be lower.

For a further radon reduction we have checked the potential of argon purification by cryo-adsorption of radon on activated carbon. The purification of argon in the gas phase is highly efficient. The purified argon has a ^{222}Rn activity of less than 0.5×10^{-6} Bq/m^3 (STP). Also the purification in the liquid phase works well, although it requires bigger carbon columns to obtain the same reduction factors. Given these results it is clear that from the radio purity point of view that both gases, nitrogen and argon, meet the specifications for GERDA.

References

[1] I. Abt et al., Letter of Intent: 'A New 76Ge Double Beta Decay, Experiment at LNGS, hep-ex/0404039.
[2] I. Abt et al., Proposal to LNGS, September 21, 2004, The Germanium Detector Array for the search of neutrinoless double beta decay in Ge-76 at the Laboratori Nazionali del Gran Sasso, http://www.mpi-hd.mpg.de/GERDA.
[3] I. Abt et al., Progress report to the Scientific Committee of the LNGS, September 2005, http://www.mpi-hd.mpg.de/GERDA.
[4] MAJORANA Collaboration 2003, nucl-ex/0311013.
[5] A. Pullia et al., IEEE Trans. Nucl. Sci. 49 (2002) 5.
[6] P.F. Manfredi et al., NIM A380 (1996) 308–311.